Tu SRS2 08

3D Elastic Full Waveform Inversion - On Land Study case

J.A. Kormann* (Barcelona Supercomputing Center), D. Marti (Institute of Earth Sciences Jaume Almera), J.E. Rodriguez (Barcelona Supercomputing Center), I. Marzan (Institute of Earth Sciences Jaume Almera), N. Gutierrez (Barcelona Supercomputing Center), M. Ferrer (Barcelona Supercomputing Center), M. Hanzich (Barcelona Supercomputing Center), J. de la Puente (Barcelona Supercomputing Center), R. Carbonell (Institute of Earth Sciences Jaume Almera), J.M. Cela (Barcelona Supercomputing Center) & S. Fernandez (REPSOL)

SUMMARY

Full Waveform Inversion is one of the most advanced processing methods that is recently reaching a mature state after years of solving theoretical and technical issues such as the non-uniqueness of the solution and harnessing the huge computational power required by realistic scenarios. In this work, we present the application of this method to a 3D on-land dataset acquired to characterize the shallow subsurface. The current study explores the possibility to apply elastic isotropic Full Waveform Inversion using only the vertical component of the recorded seismograms. One of the main challenges in this case study remains the costly 3D modeling that includes topography and free surface effects. Nevertheless, the resulting models provide a higher resolution of the subsurface structures than starting models, and show a good correlation with the available borehole measurements.

Introduction

In this work we present the application of isotropic Elastic Full Waveform Inversion (E-FWI) to a real dataset. The studied area is located within the Loranca Basin (Spain) and presents a smooth topography which is part of the challenge propose here. In order to characterize the very shallow surface, a 3D seismic data volume was acquired in a square area of 540x540 m^2. Although originally designed to perform a high resolution Travel-Time Tomography (TTT), we take advantage of the data to perform FWI. We propose to perform E-FWI because the target structures are close to the surface (< 120 m deep) making wave propagation to be mostly driven by elastic effects. On the other hand, it potentially can be more resolutive than its acoustic counterpart providing clear imaging improvements in some scenarios (Vigh et al., 2014; Raknes et al., 2015).

This dataset is part of an ongoing multidisciplinary geophysical, geological, hydrological characterization of an area which has been proposed as a possible site to host a temporal radioactive waste disposal site. Therefore, a large amount of multidisciplinary data revealing information on the underground is available including down-hole and other geophysical measurements.

In our scenario, we include free-surface effects, and consequently take topography into account. We will show that the resulting models provide a better understanding of the geological features of the area and as well as a good correlation with borehole measurements.

Theory

On one hand, we use the time-domain elastic isotropic approach for solving the elastic wave equation by means of a Fully staggered grid combined with mimetic operators (de la Puente et al., 2014)

$$
\begin{aligned}
\rho(\mathbf{x})\dot{\mathbf{v}}(\mathbf{x},t) &= \nabla \cdot \boldsymbol{\sigma}(\mathbf{x},t) + \mathbf{f}_s(\mathbf{x}_s,t), \\
\dot{\boldsymbol{\sigma}}(\mathbf{x},t) &= \mathbf{C}(\mathbf{x}) : \nabla\mathbf{v}(\mathbf{x},t)
\end{aligned}
\tag{1}
$$

where f_s is the source function at position $\mathbf{x}_s$, $\mathbf{v}$ the particle velocity, ρ the density (set as a constant), and $\boldsymbol{\sigma}$ the stress field. ths gris is deformed to accomodate the local topography.

On the other hand, the mathematical formulation of FWI consists in the minimization of a error function $E(\mathbf{m},\mathbf{m}_{real})$ (Pratt, 1999; Virieux and Operto, 2009), where $\mathbf{m}$ and $\mathbf{m}_{real}$ are the current and target model respectively. In this study we employ the normalized least-square criterion L^2 given by

$$
E_k(\mathbf{m}_k,\mathbf{m}_{real}) =
$$

$$
\frac{1}{2}\sum_{i=1}^{N}\sum_{j=1}^{n}\left[\frac{\mathbf{u}_j^i(\mathbf{x}_r,\mathbf{x}_s;\mathbf{m}_k)}{\max_j(|\mathbf{u}^i(\mathbf{x}_r,\mathbf{x}_s;\mathbf{m}_k)|)} - \frac{\mathbf{u}_j^i(\mathbf{x}_r,\mathbf{x}_s;\mathbf{m}_{real})}{\max_j(|\mathbf{u}^i(\mathbf{x}_r,\mathbf{x}_s;\mathbf{m}_{real})|)}\right]^2,
\tag{2}
$$

where N is the number of receivers, n the number of samples of each trace, $\mathbf{x}_r$ and $\mathbf{x}_s$ are the receiver and source position respectively, $\mathbf{u}(\mathbf{x}_r,\mathbf{x}_s;\mathbf{m}_k)$ and $\mathbf{u}(\mathbf{x}_r,\mathbf{x}_s;\mathbf{m}_{real})$ stand for the displacement obtained using the current model parameters at the kth iteration and the experimental dataset respectively.

Our approach for E-FWI consists in constraining the maximum offset to the longest wavelength at the current frequency in a multi-scale approach. We call this approach Dynamic Offset Control (DOC). It aims to use smaller offset for reflection data when increasing frequency. Thus, we select the offset according to

$$
Offset = V/f_0
\tag{3}
$$

where f_0 is the cut-off frequency of the low-pass filter applied to the data and V a parameter to be defined by the user. This strategy has the side effect of reducing the computational domain as we go into higher frequencies while minimizing the effect of the surface waves on the gradients. We emprically found that V equal to $\max(V_p)$ shows to be a sufficient condition. We want to stress that the computational grid

is adapted to the shortest wavelength present in the models and does not match the receiver and source grids. Besides, no part of the model has been fixed.

We apply gradient preconditioning in two steps: first we invert for $log(m)$ instead of m, and secondly we compensate for spreading by using the square of the illumination. In all our tests, it shows to be an efficient preconditioning.
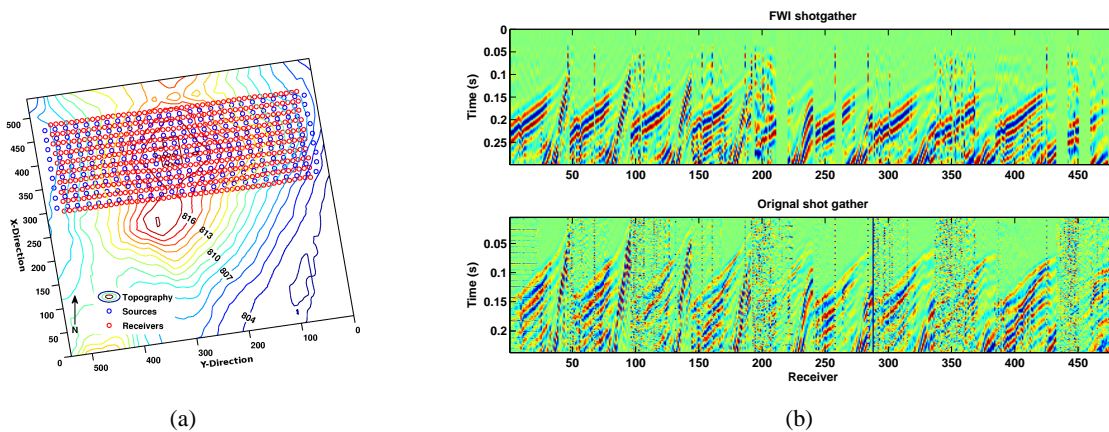

(a)   (b)

Figure 1 (a) Aquistion geometry: Topography of the zone; sources and receivers are depicted by blue and red circles respectively.(b) Shotgather normalized trace by trace: raw data (bottom) and after pre-processing and bad traces removal (top).

3D Elastic Full Waveform Inversion

The acquisition setup is shown in Fig. 1(a): it consists in 9 shooting lines and 10 recording lines of 48 geophones each. The total acquisition time is 2 s. Nevertheless, we picked the first arrivals, and apply a window of 0.2 s around them, in order to take advantage of both surface and compressional waves. The density is set to be constant as we are focusing on phase rather than to the amplitude. Dissipative effects are strongly mitigated by the misfit function and are neglected too. The starting model for V_p is obtained from (TTT) (Tryggvason et al., 2002), and half of V_p is taken as initial for V_s. We denoised the data with a band-pass filter (ranging from 10-40 Hz) applied twice, and deleted the worst traces following a mean criterion. After pre-processing, we keep 80% of the original data available (see Fig. 1(b)). The inversion strategy is summarized in Table 1, and consists in low-pass filtering, and data selection according the DOC criterion. The total computational time was 72 hours runnning on 75 nodes of Mare Nostrum supercomputer.

Frequency	15 Hz	20 Hz	25 Hz
Mesh size	40x169x169	48x201x201	56x237x237
DOC	306	230	180
Iteration	15	15	15

Table 1 Multi-grid and multi-scale parameters for 2D FWI. From top to bottom: cut-off frequency, mesh size, spatial discretization, and number of iterations.

Figure 2 presents depth slices of the velocity fields at depths 25, 50, 75, and 100 m obtained after inversion. We observe in general that the compressional velocities have been overestimated by TTT, which also could be observed on the synthetic traces obtained at the first iteration of the first frequency: predicted time arrivals are earlier than those recorded (see Fig. 3(a)). Consequently, FWI lowered velocities as observed in Fig. 2.

In Fig. 3, we present the comparison of 4 traces equally spaced along receivers line 8 of shot 813 for the final inverted models (in blue) and the seismograms predicted by the starting model (in dash green)

at frequency 25 Hz. We observe that the velocity models allow to predict much better the travel times of the recorded data. Finally, fittings of the borehole SVC6 with velocity depth profiles (located near the borehole but not at the exact position) have also been improved respect to those from the starting models: we observed a good agreement of the low-frequency content for both V_s and V_p (see Fig. 3).
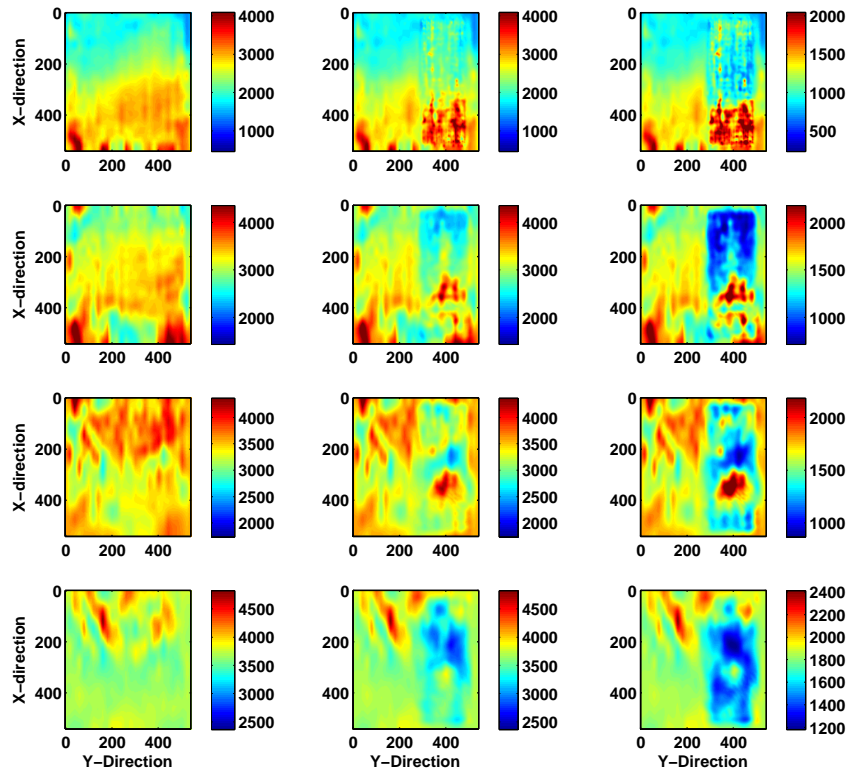

Figure 2 *Four detph slices for V_p and V_s velocities. From left to right: V_p starting model, inverted V_p, and inverted V_s. From top to bottom: depth 25, 50, 75, and 100 m.*

Conclusions

We have presented a 3D Elastic FWI successfully working on land real data including topography, using only near-source offsets. For this purpose, we have introduced an offset selection method called Dynamic Offset Control. This technique allows us to reduce the maximum aperture of each shot in FWI, hence reducing the computational cost when moving into higher frequencies, a key point for elastic inverison. E-FWI clearly improves our knowledge of the shallow subsurface structures, as observed when comparing inverted models with the borehole measurements.
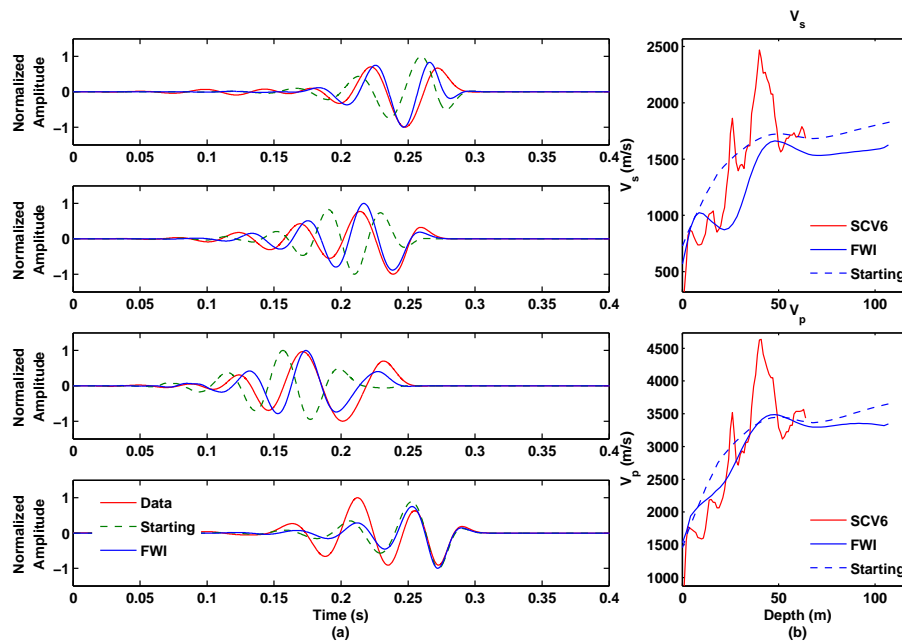
Acknowledgements

Figure 3 *(a) Shot 813 (line8, position 13): Comparison between traces from the target, starting and inverted models(red, green and blue lines respectively) for 4 receivers equally spaced along recording line. (b) Comparison with measurement from SVC6: V_s (top) and V_p (bottom).*

References

Pratt, R.G. [1999] Seismic waveform inversion in the frequency domain, Part 1: Theory and verification in a physical scale model. *Geophysics*, **64**, 888-901.

de la Puente, J., Ferrer, M., Hanzich, M., Castillo, J.E. and Cela, J.M. [2014] Mimetic seismic wave modeling including topography on deformed staggered grids. *Geophysics*, **79**(3), T125-T141.

Raknes, E.B., Arntsen, B. and Weibull, W. [2015] Three-dimensional elastic full waveform inversionusing seismic data from the Sleipner area. *Geophysical Journal International*, **202**, 1877-1894.

Tryggvason, A., Rögnvaldsson, S. and Flovenz, Ó.G.. [2002] Three-dimensional imaging of P- and S-wave velocity structure and earthquake locations beneath southwest Iceland. *Geophysical Journal International*, **171**(5), 848-866.

Vigh, D., Jiao, K., Watts, D. and Sun, D. [2014] Elastic full-waveform inversion application using multicomponent measurements of seismic data collection. *Geophysics*, **79**(2), R63-R77.

Virieux, J. and Operto, S. [2009] An overview of full-waveform inversion in explorat ion geophysics. *Geophysics*, **74**, WCC127-WCC152.